

The Shape of Word Embeddings: Recognizing Language Phylogenies through Topological Data Analysis

Ondřej Draganov

Institute of Science and Technology Austria (ISTA) Dept. of Computer Science
Am Campus 1, 3400
Klosterneuburg, Austria
ondrej.draganov@ist.ac.at

Steven Skiena

Dept. of Computer Science
Stony Brook University
Stony Brook, NY 11794-2424 USA
skiena@cs.stonybrook.edu

Abstract

Word embeddings represent language vocabularies as clouds of d -dimensional points. We investigate how information is conveyed by the general shape of these clouds, outside of representing the semantic meaning of each token. Specifically, we use the notion of persistent homology from topological data analysis (TDA) to measure the distances between language pairs from the shape of their unlabeled embeddings. We use these distance matrices to construct language phylogenetic trees over 81 Indo-European languages. Careful evaluation shows that our reconstructed trees exhibit strong similarities to the reference tree.

An interesting aspect of the topological analysis of word embeddings we consider here is that it makes no assumption or use of translation pairs, surface similarities between words, or cognate pairs. Word embeddings are treated as *unlabeled* sets of points, shorn of any binding to corresponding tokens. TDA compares the relative *shape* of word embeddings in terms of structural properties like components and holes. That we will demonstrate even a weak ability to reconstruct language phylogenies through TDA is surprising, and suggests that there are hitherto unknown structures reflected in word embeddings that go beyond the semantics of individual words.

Our major contributions in this paper include:

1 Introduction

Word embeddings are well-established objects of interest in natural language processing, being d -dimensional vector representations that capture the semantics of each vocabulary word. The vocabulary of language L can thus be viewed as a cloud of points, whose geometric and structural properties encode considerable information about the language. In this paper, we will demonstrate that, even after disassociated from their bindings to particular words, the “shape” of these point clouds reflect the history of the languages they represent, by using techniques from *topological data analysis* (TDA), a field studying spatial aspects of data.

The history of language evolution is typically studied by identifying *cognate* word pairs of languages L_1 and L_2 , namely homologous word forms inherited from the common ancestor of these languages. Cognates typically share some level of surface-form similarity between them, with language pairs sharing more cognates presumed to be more closely related. The identification of cognate pairs traditionally requires extensive labor by skilled linguists, although computational methods for detecting cognate pairs are emerging (Kondrak, 2001; Lefever et al., 2020; St Arnaud et al., 2017).

- *Comparing the Shapes of Word Embeddings using Topological Data Analysis (TDA)* – Through our experimental setup on language phylogeny reconstruction, we will test two related properties concerning the geometric structure of word embeddings. First, we will show that the shape of the unlabeled word embedding of a language carries information about its history and structure. Second, we show that this information can be at least partially recovered through persistent homology, a standard tool in TDA.
- *Statistical Evaluation of TDA-Based Language Phylogenies* – Evaluating the information content of language distance matrices inferred using TDA is best done by converting these matrices into phylogenetic trees, and then assessing the quality of these trees against a reference standard. Representative trees constructed using our methods are presented in Figure 2. We perform an extensive study evaluating the accuracy of TDA distance matrices derived from two different types and three different dimensions of persistence diagram, compared using four different distances be-

tween persistence diagrams. Each of these 24 different TDA matrices was evaluated on two popular tree construction algorithms (UP-GMA and neighbor joining) and compared against a gold-standard language tree (from Ethnologue) under six different tree-similarity metrics.

Certain matrices and metrics prove less capable of encoding or recognizing the structural similarities inherent in word embeddings. But permutation tests show that for 484 out of 864 combinations of parameters, the quality of the reconstructed trees were significant to the 0.05-level, and many substantially stronger than that. Even stronger bounds come in the number of standard deviations our TDA trees are closer to the gold-standard tree compared to the mean statistical background. Many of our TDA-based trees sit from four to seven σ from the mean. Under assumptions of normality, the maximum achieved 6.87σ corresponds to a Bonferroni-corrected p -value of 2.77×10^{-9} of seeing a result like this by chance.

- *A Case Study in Topological Data Analysis* – TDA provides a relatively new set of tools for data science able to capture features often missed by more traditional approaches. Due to the general framework it provides, there are many parameters to choose from—selecting the filtration function on data, dimension of studied features, distance notion between the extracted features, etc.—and a priori no obvious canonical choices. Our analysis on word embeddings represents a rigorous evaluation for an interesting use-case of this technology. We demonstrate that TDA methods successfully capture aspects of the shape of language embeddings. Our analysis shows that persistence diagrams in dimensions 2, which are not that often used in large high-dimensional data because of the expense in constructing them and difficulty to interpret them, yield statistically-strong results in our experiments, in some cases outperforming dimensions 0 and 1.

We presume a reader from computational linguistics, with a basic familiarity with the concepts and literature of word embeddings and language phylogenies, but no prior exposure to topologi-

cal data analysis. Our paper is organized as follows. Important TDA concepts like persistence diagrams and the Vietoris-Rips complex are reviewed in Section 2. Algorithms for constructing language phylogenies from distance matrices and evaluating the resulting trees are presented in Section 3. We describe our TDA-based analysis pipeline in Section 4 with computational results reported in Section 5.

Our primary goal in this work is to initiate the study of the shape of languages via word embeddings, not to advance the state-of-the-art in language phylogeny reconstruction. Indeed, cognate-based analysis should clearly dominate our unlabeled point methods except perhaps in pathological situations, such as completely undeciphered written languages. But we do believe that our new TDA-based tools hold promise for richer computational language analysis, and raise interesting question about which properties in language-space the topological features we employ correspond to.

2 Topological Data Analysis

Topological data analysis (TDA) is a growing field that applies methods developed for studying shapes to data, both geometrical and abstract, to extract features that are often not captured by classical approaches of data science. In the case of points or vectors in 2- or 3-dimensional space, we observe certain patterns like clusters of points, empty spaces surrounded by points (voids) or tunnels in 3D. TDA studies such structures in a quantitative way.

To keep the explanation intuitive, we stay with low dimensional point sets, but the general framework is limited neither by dimension of the data nor by the Euclidean metric—indeed, we use 300-dimensional word embeddings and impose both Euclidean and cosine metrics. For a gentle introduction to TDA see (Edelsbrunner, 2014). For more technical details, see (Edelsbrunner and Harer, 2010). For applications of TDA to a wide variety of real-world data, see the database of non-theoretical uses of topology (Giunti et al., 2022).

2.1 Persistent homology

We first describe the idea of persistent homology in a simple intuitive setting—consider a data set of points in a Euclidean plane. To define the ‘shape’ of such a set, choose a radius, place a disk of that radius centered at each point, and consider the union

of the disks; see Figure 1. Two simple descriptors for such a shape are the number of connected components and the number of holes. These are *Betti numbers*¹ of the shape, β_0 and β_1 , respectively—a notion formally defined by *homology*, a tool in the mathematical field of algebraic topology; see, e.g., (Hatcher, 2002).

For different radii of the disks, we get different Betti numbers. Consider growing the radius from zero to infinity. We can plot the Betti numbers depending on the radius, and treat the curves, $\beta_0(r)$, $\beta_1(r)$, as descriptors for the shape of our point set. The problem is that such a curve can differ a lot when we slightly perturb the points. For a stable descriptor, we turn to *persistent homology*, which, in addition, pairs the *birth* and *death* radii of each component or hole. For example, there is a minimum radius r_b for which the disks enclose a space in the plane, separating it from its surroundings. This is the birth radius of a hole. Then there is a larger minimum radius r_d , for which the area we previously enclosed is fully covered by the disks. The interval $[r_b, r_d)$, often called a *bar*, is a single feature recorded by persistent homology. It is the interval of radii during which this particular hole contributes “plus one” to the Betti number β_1 .

We collect all such intervals. Each interval is described by its two endpoints, so we can plot them all in a scatter plot with axes “birth radius” and “death radius”; see Figure 1(c). This plot is the *persistence diagram* of the data point set. For a point set in a plane, we get two persistence diagrams: one for components of connectivity, i.e., the 0-dimensional features contributing to β_0 , and one for ‘holes’ or ‘loops’, i.e., the 1-dimensional features contributing to β_1 . Usually we plot both in the same figure, separating them by color and shape of the markers.

When we increase the dimension of the data, we can have more different kinds of features. A 2-dimensional feature is an uncovered space completely surrounded by covered space—like a hole completely inside a Swiss cheese. Analogously to loops in 3D, in higher dimensional data, a 2-dimensional feature would not be a completely enclosed space, but rather a drawing of a 2-dimensional sphere that cannot be contracted into a point. Even though our actual data is 300-

dimensional, we only consider features of dimension 0, 1 and 2, mainly for computational reasons. Examples of diagrams used in our analysis are provided in Appendix Figure 9.

Persistent homology is stable. That is, if the data points are perturbed a bit, the points on the persistence diagrams are also only perturbed a bit (Cohen-Steiner et al., 2007). Note that points can appear and disappear on the diagonal of a persistence diagram in the process. To properly state the stability, we need to define a notion of distance that reflects that. Usually the stability is phrased with respect to the bottleneck distance or 1-Wasserstein distance—see Section 2.3 for the definitions.

2.2 Vietoris-Rips complex

For low-dimensional Euclidean data, persistent homology is usually computed using Delaunay complexes with alpha filtration. From the topological perspective, those complexes exactly reflect the spaces of growing disks. However, computing Delaunay complexes is not practically viable for data in dimensions beyond ~ 10 . A widely used alternative is the Vietoris-Rips complex. It can be constructed from any distance matrix, and for Euclidean data offers a good approximation of the alpha filtration. Its low-dimensional persistent homology can be computed efficiently, and a fast implementation is readily available.

Given an $n \times n$ distance matrix D , and a radius $r > 0$, the *Vietoris-rips complex*, $VR_r(D)$, is the flag complex of all the edges $\{i, j\}$ with $D_{i,j} \leq r$. That is, $\sigma \subseteq [n] = \{1, \dots, n\}$ is a face of $VR_r(D)$ iff $D_{i,j} \leq r$ for all $\{i, j\} \subseteq \sigma$. As the radius grows to infinity, the complex grows to become the full-simplex $2^{[n]}$ whose size grows exponentially with respect to n . The reason that this is not a problem for computations is that the full complex need not be computed to obtain persistent homology. Firstly, only edges, triangles and tetrahedra are relevant when we only care for 0-, 1- and 2-dimensional persistent homology, secondly, there exists a radius cut-off after which the homology is guaranteed to be trivial, and finally, the relevant structures can be used implicitly rather than stored explicitly in memory. For more details see (Bauer, 2021).

2.3 Distances between persistence diagrams

In this section, we describe several established notions of distances between persistent diagrams. The list we use is by no means exhaustive—see, e.g., (Ali et al., 2023) for a survey of methods, and (Car-

¹The formal definition of Betti numbers depends on the choice of coefficients for homology. We use the field of size two, $\mathbb{Z}/2\mathbb{Z}$, which is the standard choice for persistent homology.

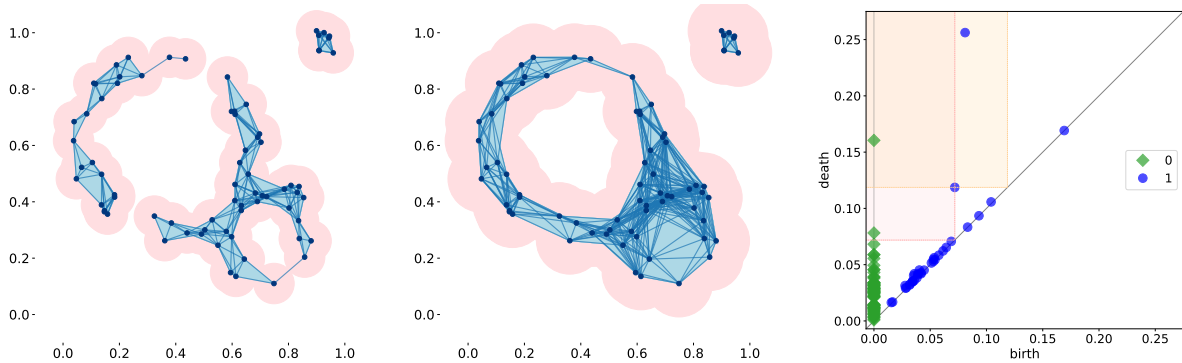


Figure 1: Unions of disks centered at data points in a Euclidean plane define a ‘shape’ that varies with the radius of the disks. Persistent homology studies different types of ‘gaps’ within this growing shape, e.g., 0-dimensional gaps between components of connectivity, and 1-dimensional holes within the shape. Each such feature is born at some radius, and dies at some later radius, spanning an interval $[r_b, r_d]$. Those intervals are summarised in a persistence diagram—each interval is represented by a dot with coordinates (r_b, r_d) . The *left* and *middle* figures show the growing disks around a point set $A \subseteq \mathbb{R}^2$ with the radii of the endpoints of an interval $[r_b, r_d] = [0.072, 0.119]$, as well as the Vietoris-Rips complexes $VR_{r_b}(A)$, $VR_{r_d}(A)$. On the *right* is the persistence diagram of the growing disks with highlighted blocks corresponding to radii r_b, r_d .

rière et al., 2020) for an approach unifying many of those methods under a common framework. We chose four distances that are widely used in theory or in applications and have readily available implementations. Two of those are defined directly on the diagrams, while the other two first vectorize each diagram and then compare the vectors with the standard Euclidean metric.

We fix two persistent diagrams, PD_1 and PD_2 , describing topological features of the same dimension. An element r of PD_i is a point in a plane representing an interval, and we will denote its endpoints by $r = [r_b, r_d]$ for “birth” and “death”.

Bottleneck distance. The first distance that was proved to be stable (Cohen-Steiner et al., 2007) is the *bottleneck distance*, which is defined as “the biggest difference for the best matching”. A *matching*, \mathcal{M} , between two persistence diagrams is a pairing of the points they contain, with an added flexibility—we can match points with any points on the diagonal. That is, if $(r, s) \in \mathcal{M}$, then either $r \in PD_1$ and $s \in PD_2$ or only one of those holds and the other element is $[x, x)$ for some number x . The bottleneck distance between PD_1 and PD_2 is then

$$W_\infty(PD_1, PD_2) = \inf_{\mathcal{M}} \max_{(r,s) \in \mathcal{M}} \max\{|r_b - s_b|, |r_d - s_d|\}.$$

Bottleneck distance is a classical notion, but it is computationally costly since we have to search the space of matchings.

(Sliced) Wasserstein distance. The maxima in the bottleneck distance can be seen as l_∞ -norm, which suggests that they can be replaced by l_p norms, for various $p \in \mathbb{N}$, to get different notions of distances. In particular, replacing both maxima by l_1 -norm, we get *1-Wasserstein distance* between persistence diagrams:

$$W_1(PD_1, PD_2) = \inf_{\mathcal{M}} \sum_{(r,s) \in \mathcal{M}} |r_b - s_b| + |r_d - s_d|$$

This distance takes each interval in either diagram into consideration, not just the worst match as the bottleneck distance. It is stable with respect to data perturbations (Cohen-Steiner et al., 2010; Skraba and Turner, 2023). In our analysis, we use a computationally more viable variant—*sliced Wasserstein distance* which approximates 1-Wasserstein distance (Carrière et al., 2017).

Persistence image. Rather than directly comparing the diagrams, we can first transform each into a vector and then compare the vectors. One approach to vectorize a diagram is to blur the points and then treat the plot as a raster image, called *persistence image* (Adams et al., 2017). Persistence images are stable and approximate the 1-Wasserstein distance.

Persistence images are easy to compute, but there is several parameters we need to fix—the size of the pixels and the grid, the σ -parameter of the Gaussians, and the weight function controlling the heights of the Gaussians based on the $d - b$ parameter.

Bars statistics. A somewhat naive, but surprisingly successful vectorization is to collect several simple statistics of the collection of dots (also called bars) in the persistence diagram (Pun et al., 2022; Cang et al., 2015; Ali et al., 2023). We used 40 numbers—10 statistics for 4 values. For each dot, (b, d) , the 4 values are birth, death, persistence and midpoint, i.e., $b, d, d - b$ and $\frac{d+b}{2}$, respectively. The 10 statistics are: median, standard deviation, interquartile range, full range, 10th percentile, 25th percentile, 75th percentile, 90th percentile, and entropy. To compare two diagrams, we compute the Euclidean distance between the vectorizations.

This vectorization method misses theoretical guarantees like the stability, but is very easy to compute, the meaning of the features is clear, and may mitigate the negative effects of outliers.

3 Constructing/Evaluating Phylogenies

We emphasize that reconstructing language phylogenies is an enormous area within computational linguistics, and space does not permit us to make a substantial survey of work in this field. See (Dunn, 2015; Pereltsvaig and Lewis, 2015; Pompei et al., 2011) for recent reviews of this literature. We are interested in phylogeny reconstruction primarily as a task to evaluate the extent to which the unlabeled topological “shape” of word embeddings retain and reflect broader properties of the underlying languages. Thus we use standard distance-based tree reconstruction algorithms (unweighted pair group method with arithmetic means (UPGMA) and neighbor joining) (Gusfield, 1997) and tree similarity metrics detailed below.

3.1 Data

Our study requires two types of data over a large set of languages: (a) a source of directly comparable, high quality word embeddings, and (b) a ground-truth reference phylogenetic tree reflecting the origin and relative similarity of languages in this set. We limit our attention here to the broad family of Indo-European languages for this study.

The historical origin of languages has been extensively studied, and much is known, but debate remains vigorous even for the Indo-European languages we study here (Gray and Atkinson, 2003; Pereltsvaig and Lewis, 2015; Longobardi et al., 2013). The reference tree we use comes from Ethnologue (<https://www.ethnologue.com>), which is the most widely consulted inventory of the

world’s languages (Lewis et al., 2024). First published in 1951 and now in its 26th edition, Ethnologue currently records data about 7,168 living languages. Although there is no universal agreement on language origins (see e.g. (Hammarström, 2015) for a critique of Ethnologue), it provides a broadly acceptable reference tree for our evaluation purposes, particularly for the major Indo-European languages we consider here.

FastText (Bojanowski et al., 2017) (<https://fasttext.cc/>) provides a set of pre-trained, 300-dimensional word embeddings for 157 languages, trained on Common Crawl and Wikipedia. There are 81 Indo-European languages that appear in the Ethnologue reference tree and also have pre-computed FastText embeddings. To protect against the risk that low-resource languages might have less reliable embeddings, we will also evaluate filtrations to the most popular 30 and 50 languages—see Section 4. The Ethnologue reference trees for all filtrations are provided for inspection in Appendix Figure 7.

3.2 Constructing Algorithmic Phylogenies

In this paper, we experiment with two popular agglomerative hierarchical clustering algorithms for reconstructing phylogenetic trees from a pairwise distance matrix, $d(\cdot, \cdot)$. We start with each language as an individual cluster, and then we connect two “closest” clusters in each step. The difference is what “closest” means for each of the algorithms:

Unweighted Pair Group Method with Arithmetic Mean (UPGMA). The UPGMA method (Sneath and Sokal, 1973) approximates distances between clusters as the average distance between the elements: for clusters A, B , the distance is

$$d(A, B) := \frac{1}{|A| \cdot |B|} \sum_{\substack{a \in A \\ b \in B}} d(a, b).$$

Starting with singleton clusters, in each step it merges the two closest clusters into one.

Neighbor Joining (NJ). The NJ method (Saitou and Nei, 1987) defines distances between clusters, $D(\cdot, \cdot)$, inductively through a merging process. Let C be the collection of current clusters. For each cluster, $c \in C$, define

$$\alpha(c) := \frac{1}{|C| - 2} \sum_{\substack{d \in C \\ d \neq c}} D(c, d).$$

Find a pair $a, b \in C$ minimizing $D(a, b) - \alpha(a) - \alpha(b)$. We replace a, b by the union, $a \cup b$, and define the new distances $D(a \cup b, d) := (D(a, d) + D(b, d) - D(a, b))/2$ for each other d .

Figure 2 gives examples of reconstructed and reference trees.

4 Analysis Pipeline

In this section we describe our pipeline to go from the embeddings of languages to a phylogenetic tree, list the parameter choices at each step, and provide details about the implementation.

We start with a set of embeddings of languages. For each language, we compute a distance matrix between its words. For each such matrix, we use persistent homology and get a set of persistent diagrams. Computing distances between the persistent diagrams yields a distance matrix labeled by languages. From this language distance matrix we finally construct a phylogenetic tree.

Language embeddings. We work with language embeddings from FastText (Grave et al., 2018). We filter the data in two ways. Firstly, we use the $V = 10,000$ most frequent tokens of each language. Secondly, we only choose a subset of the languages to work with. Because low-resource languages may skew our analysis, we filter the languages by the number of Wikipedia articles², and consider the first 30, 50 or all 81 Indo-European languages.

Embedding distance matrices. The persistent homology pipeline we use takes a distance matrix as the input. Therefore, for each language, we generate a $V \times V$ matrix, each entry being the distance between two 300-dimensional vectors, u, v . We use two different notions of distances—this is the second parameter—either the standard Euclidean distance, $\|u - v\|$, or the cosine distance, $1 - a \cdot b / (\|a\| \cdot \|b\|)$, which is often used in language processing.

Persistence diagrams. For the embedding distance matrix of each language, we compute the persistence diagram of its Vietoris-Rips complex, as described in Section 2.1, using an efficient implementation of this computation, Ripser (Bauer, 2021)³. In this step, we choose the dimension of the topological features to use—either 0, 1 or 2.

Languages distance matrix. From the set of persistence diagrams, we get a single distance matrix representing the proximity of language pairs. The distance between diagrams is one of the four described in Section 2.3—this is the fourth parameter.

We use bottleneck distance implementation from GUDHI library⁴ (François, 2016), and slice Wasserstein and persistence image implementations from persim Python library⁵. Bar statistics are computed directly.

For the bars statistics, in dimension 0 we only use the death, d , value, as $b = 0$ for all dots. That is, the vectorization is 10-dimensional in this case rather than 40-dimensional as in the other cases.

Tree construction. Finally, we construct a phylogenetic tree based on the language distance matrix. We try two different approaches. First, we construct the tree with either of the two agglomerative clustering algorithms described in Section 3—neighbor joining (NJ) or unweighted pair group method with arithmetic mean (UPGMA). Both of those algorithms are implemented in biopython package⁶ under DistanceTreeConstructor class.

We also conducted a second set of experiments to allay concerns about the difference in height/topology between algorithm and reference trees, by fixing our algorithmic trees to have the same unlabeled topology as the reference tree. The random labeling whose tree distances between language pairs best correlated with the TDA-based distances between language word embeddings is taken as our algorithmically-designed tree, which can then be compared to the Ethnologue tree using the distance metrics previously defined. Consistent with the results to be reported below, we perform substantially better than chance for almost all combinations of TDA variant and tree distance metric, typically by two or more standard deviations from the mean. Details are presented in the Appendix.

5 Experiments

5.1 Evaluating Phylogenetic Trees

To compare the reference Ethnologue tree R to each phylogenetic tree T constructed using language distances inferred by TDA, we employ six different tree distances, using implementations from the R package TreeDist version 2.6.3.

²https://meta.wikimedia.org/wiki/List_of_Wikipedias, extracted on November 8, 2023

³<https://github.com/Ripser/ripser>

⁴<https://gudhi.inria.fr>

⁵<https://github.com/scikit-tda/persim>

⁶<https://biopython.org/wiki/Phylo>

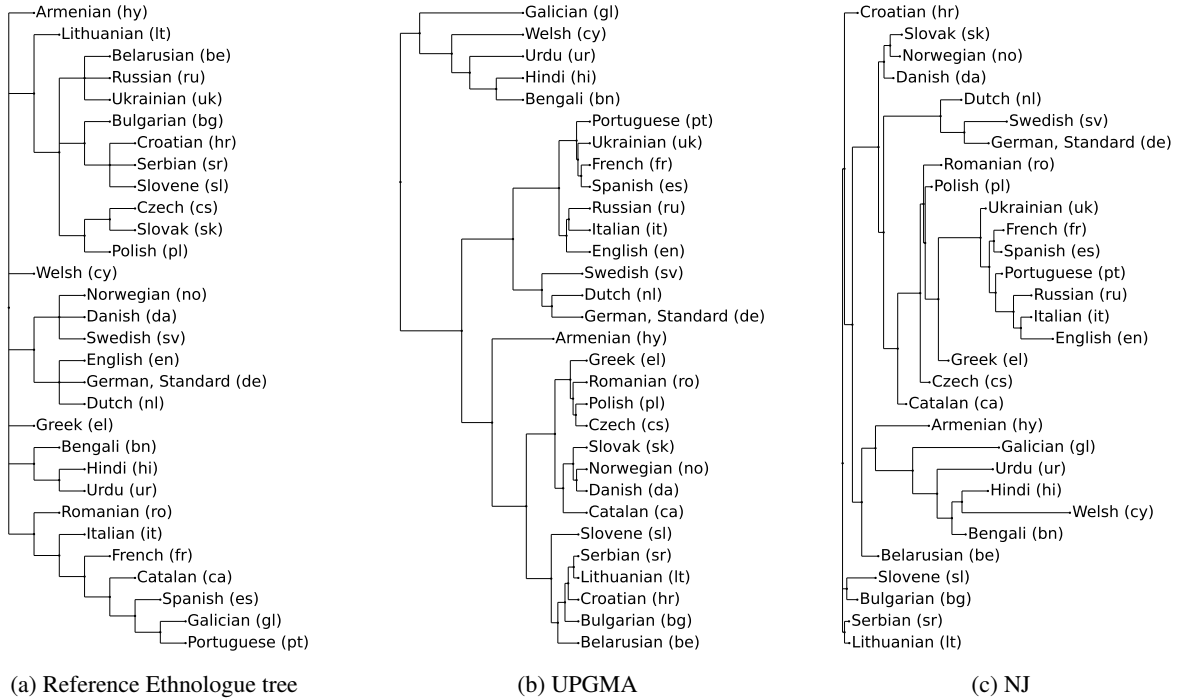


Figure 2: The 30-language reference Ethnologue tree with representative UPGMA and NJ reconstructed trees using TDA (here 2-dimensional persistent homology using Euclidean distance and inferred distances between languages based on bars statistics between the persistent diagrams). Although far from perfect agreement, the reconstructed trees captures many meaningful language subgroups; for UPGMA, e.g. (i) clusters of Balto-Slavic languages (*sl*, *sr*, *lt*, *hr*, *bg*, *be*), (ii) the Romance Italo-Western group (*pt*, *fr*, *es*, *it*) mixed with Germanic languages (*de*, *nl*, *en*, *sv*), while (iii) the more distant Indo-Aryan languages (*bn*, *hi*, *ur*) are clustered and well-separated.

These include (i) path distance (Farris, 1969; Steel and Penny, 1993), (ii/iii) Jaccard-Robinson-Foulds distance for $k = 1$ and $k = 2$ (Nye et al., 2005; Böcker et al., 2013), (iv) matching split distance (Bogdanowicz and Giaro, 2012; Lin et al., 2012), and (v/vi) the phylogenetic and clustering information distances (Smith, 2020). These distances are described formally in Appendix Section A.2.

To assess whether the reconstructed trees capture part of the real phylogeny, we evaluate them in terms of leaf label permutations—comparing the distance $d(T, R)$ between the algorithmic tree T and reference R to the distribution of $d(T', R)$, where T' is obtained from T by shuffling the leaf labels.

For each tree, T , constructed by UPGMA or NJ algorithm, we performed 100,000 permutations of its leaf labels. For each permuted tree, we measure the six tree distances to the reference Ethnologue tree with the corresponding number of leaves—30, 50 or 81. Then, separately for each of the six tree distances, we identify where in this distribution of distances $d(T, R)$ lies. The measure of success is to check how many random permutations did worse

than T . Those numbers are clustered towards the upper end—for 484 out of 864 distributions, at least 95,000 (95%) of the permutations are further from R than T is.

5.2 Results

Figure 3 is the primary result in this paper, presenting the results of evaluations of 144 different algorithmic tree reconstructions using TDA, each evaluated on six different tree similarity measures, for a total of 864 different points. By employing permutation tests, we can map each such point to a significance level, expressed in terms of (a) the fraction of random samples dominated by the reconstructed tree or (b) the number of standard deviations the reconstructed tree sits from the mean value over 100,000 random trees; the options are tightly correlated. Figure 3 summarises (b); analogous figure for (a) is in Appendix Figure 8.

Further summary of these results is in Figure 4. The cumulative distribution plots show the fraction of experimental conditions which satisfy a given permutation test p -value. With respect to this value, 484 out of the 864 conditions proved significant to at least the 0.05-level. Of these, 255 were signifi-

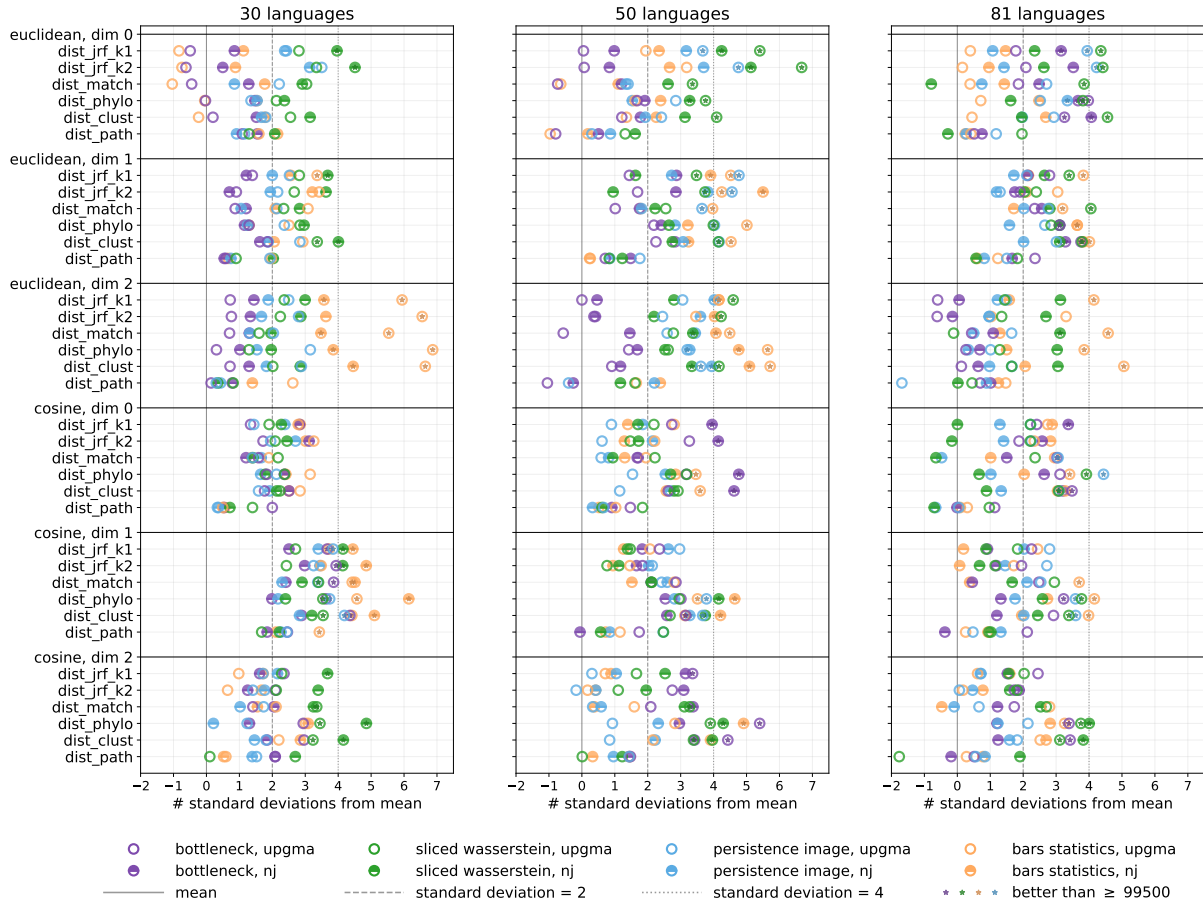


Figure 3: The statistical significance of TDA trees for 30, 50, and 81 languages against the Ethnologue reference for trees reconstructed by UPGMA and NJ for each combination of parameters described in Section 4. Each dot represents the distance of a single reconstructed tree to the reference, and its position shows how many standard deviations from the mean it lies in the distance distribution over 100,000 random permutations of the tree’s leaves.

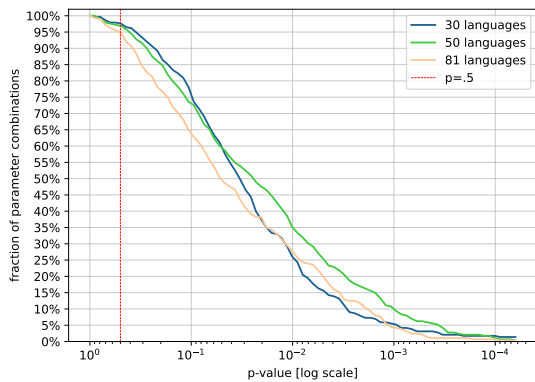


Figure 4: The fraction of parameter combinations (out of 288) in Figure 3 that are bested by at most $p \cdot 100,000$ permutations.

cant to at least 0.01, 57 to at least 0.001, and 10 to 0.0001. In one case the algorithmic tree dominated all $t = 100,000$ random permutations evaluated. Our statistically strongest results came when using $n = 50$ languages: large enough to encode

topologies hard to find by chance while avoiding low resource languages with poorly shaped embeddings. Twice as many tests for UPGMA trees (114) were significant to the 0.005-level as NJ trees (63), demonstrating that better combinatorial optimization leads to more significant phylogenies. Detailed breakdowns are provided in Tables 1, 2, 3, 4 in the Appendix.

That our best tree beats all trial t permutations in our experiment implies it is significant beyond the $1/t$ level. By measuring the quality score of each tree with respect to each distance in terms of the number of standard deviations above its random background mean and assuming normality, we can obtain a p -value associated with each such z -score. The maximum achieved 6.87σ corresponds to a Bonferroni-corrected p -value of 2.77×10^{-9} . Coupled with all other presented permutation test results, clearly TDA is picking up real signal from the shape of word embeddings.

Limitations

In this paper, we have demonstrated that TDA methods are capable of reconstructing a real (albeit somewhat weak) signal about language structure and history from unlabeled word embeddings.

However, there are reasons to be optimistic that the strength of this signal may be increased with further research and experience. We note that our TDA analysis is “blind”, with no statistical normalizations of numerical range across the different language embeddings. Orthogonal transformations preserve distances and angles, so they do not influence persistent homology, but scaling does change Euclidean distances, and translation can change the cosine distances.

Outlier points may impact persistent homologies in misleading ways. For example the “U-” token in the English language embedding skewed the Euclidean 0-dim homology, even though it was completely isolated. This motivates the question of whether we can preprocess data to eliminate clear outliers before analysis.

There is somewhat of a gap between the low-dimensional persistent homologies of dimensions $0 \leq d \leq 2$ which are computationally accessible and the 300-dimensional word vectors we analyze. In hopes of capturing more of the higher order behavior of high-dimensional data, data is often first reduced to fewer dimensions before persistent homology is applied. Standard methods like PCA, t-SNE or U-Map can be used to reduce dimension to ~ 10 or ~ 50 .

We restrict our attention here to one popular but particular set of GloVe embeddings, without evaluating other methods such as word2vec, which are geometrically quite different and may in principle have even better topological properties. There are also reasonable questions of whether our results may strengthen if we used a different reference tree than provided by Ethnologue which is difficult to compare to: it is unrooted, non-binary, and very flat.

Our results demonstrate that TDA invariants capture properties of natural languages, but it remains completely open about what aspects of language they are keying on. What do tunnels and voids in embedding space tell us about languages? An interesting possible future work revolves around optimizing the parameters to compare persistence diagrams for informative regions to try to identify which structures have concrete linguistic meaning.

References

- Henry Adams, Tegan Emerson, Michael Kirby, Rachel Neville, Chris Peterson, Patrick Shipman, Sofya Chepushtanova, Eric Hanson, Francis Motta, and Lori Ziegelmeier. 2017. Persistence images: A stable vector representation of persistent homology. *Journal of Machine Learning Research*, 18.
- Dashti Ali, Aras Asaad, Maria-Jose Jimenez, Vidit Nanda, Eduardo Paluzo-Hidalgo, and Manuel Soriano-Trigueros. 2023. A survey of vectorization methods in topological data analysis. *IEEE Transactions on Pattern Analysis and Machine Intelligence*, 45(12):14069–14080.
- Ulrich Bauer. 2021. Ripser: efficient computation of Vietoris-Rips persistence barcodes. *J. Appl. Comput. Topol.*, 5(3):391–423.
- Sebastian Böcker, Stefan Canzar, and Gunnar W. Klau. 2013. The generalized robinson-foulds metric. In *Algorithms in Bioinformatics*, pages 156–169, Berlin, Heidelberg. Springer Berlin Heidelberg.
- Damian Bogdanowicz and Krzysztof Giaro. 2012. Matching split distance for unrooted binary phylogenetic trees. *IEEE/ACM Transactions on Computational Biology and Bioinformatics*, 9(1):150–160.
- Piotr Bojanowski, Edouard Grave, Armand Joulin, and Tomas Mikolov. 2017. Enriching word vectors with subword information. *Transactions of the Association for Computational Linguistics*, 5:135–146.
- Zixuan Cang, Lin Mu, Kedi Wu, Kristopher Opron, Kelin Xia, and Guo-Wei Wei. 2015. A topological approach for protein classification. *Computational and Mathematical Biophysics*, 3(1).
- Mathieu Carrière, Frédéric Chazal, Yuichi Ike, Théo Lacombe, Martin Royer, and Yuhei Umeda. 2020. Perslay: A neural network layer for persistence diagrams and new graph topological signatures. In *International Conference on Artificial Intelligence and Statistics*, pages 2786–2796. PMLR.
- Mathieu Carrière, Marco Cuturi, and Steve Oudot. 2017. Sliced Wasserstein kernel for persistence diagrams. In *Proceedings of the 34th International Conference on Machine Learning*, volume 70 of *Proceedings of Machine Learning Research*, pages 664–673. PMLR.
- David Cohen-Steiner, Herbert Edelsbrunner, and John Harer. 2007. Stability of persistence diagrams. *Discrete Comput Geom*, 37:103–120.
- David Cohen-Steiner, Herbert Edelsbrunner, John Harer, and Yuriy Mileyko. 2010. Lipschitz functions have l_p -stable persistence. *Foundations of Computational Mathematics*, 10:127–139.
- Michael Dunn. 2015. Language phylogenies. *The Routledge handbook of historical linguistics*, pages 190–211.

- Herbert Edelsbrunner. 2014. *A Short Course in Computational Geometry and Topology*. Springer Cham.
- Herbert Edelsbrunner and John Harer. 2010. *Computational Topology: An Introduction*. American Mathematical Society.
- James S. Farris. 1969. [A Successive Approximations Approach to Character Weighting](#). *Systematic Biology*, 18(4):374–385.
- Godi François. 2016. Bottleneck distance. In *GUDHI User and Reference Manual*. GUDHI Editorial Board.
- Barbara Giunti, Jānis Lazovskis, and Bastian Rieck. 2022. DONUT: Database of Original & Non-Theoretical Uses of Topology. <https://donut.topology.rocks>.
- Edouard Grave, Piotr Bojanowski, Prakhar Gupta, Armand Joulin, and Tomas Mikolov. 2018. Learning word vectors for 157 languages. In *Proceedings of the International Conference on Language Resources and Evaluation (LREC 2018)*.
- Russell D. Gray and Quentin D. Atkinson. 2003. Language-tree divergence times support the Anatolian theory of Indo-European origin. *Nature*, 426(6965):435–439.
- Dan Gusfield. 1997. *Algorithms on strings, trees, and sequences: Computer science and computational biology*. Cambridge University Press.
- Harald Hammarström. 2015. "Ethnologue" 16/17/18th editions: A comprehensive review. *Language*, 91:723–737.
- Allen Hatcher. 2002. *Algebraic topology*. Cambridge University Press, Cambridge.
- Grzegorz Kondrak. 2001. [Identifying cognates by phonetic and semantic similarity](#). In *Second Meeting of the North American Chapter of the Association for Computational Linguistics*.
- Els Lefever, Sofie Labat, and Pranaydeep Singh. 2020. [Identifying cognates in English-Dutch and French-Dutch by means of orthographic information and cross-lingual word embeddings](#). In *Proceedings of the Twelfth Language Resources and Evaluation Conference*, pages 4096–4101, Marseille, France. European Language Resources Association.
- M. Paul Lewis, Gary F. Simons, and Charles D. Fennig. 2024. *Ethnologue: The languages of the world*. SIL International, Dallas.
- Yu Lin, Vaibhav Rajan, and Bernard M.E. Moret. 2012. [A metric for phylogenetic trees based on matching](#). *IEEE/ACM Transactions on Computational Biology and Bioinformatics*, 9(4):1014–1022.
- Giuseppe Longobardi, Cristina Guardiano, Giuseppina Silvestri, Alessio Boattini, and Andrea Ceolin. 2013. Toward a syntactic phylogeny of modern indo-european languages. *Journal of Historical Linguistics*, 3(1):122–152.
- Tom M.W. Nye, Pietro Liò, and Walter R. Gilks. 2005. [A novel algorithm and web-based tool for comparing two alternative phylogenetic trees](#). *Bioinformatics*, 22(1):117–119.
- Asya Pereltsvaig and Martin W Lewis. 2015. *The Indo-European Controversy*. Cambridge University Press.
- Simone Pompei, Vittorio Loreto, and Francesca Tria. 2011. On the accuracy of language trees. *PloS one*, 6(6):e20109.
- Chi Seng Pun, Si Xian Lee, and Kelin Xia. 2022. Persistent-homology-based machine learning: a survey and a comparative study. *Artificial Intelligence Review*, 55(7):5169–5213.
- D.F. Robinson and L.R. Foulds. 1981. [Comparison of phylogenetic trees](#). *Mathematical Biosciences*, 53(1):131–147.
- Naruya Saitou and Masatoshi Nei. 1987. The neighbor-joining method: a new method for reconstructing phylogenetic trees. *Molecular biology and evolution*, 4(4):406–425.
- Primoz Skraba and Katharine Turner. 2023. [Wasserstein stability for persistence diagrams](#). *arXiv*, page 2006.16824.
- Martin Ross Smith. 2020. [Information theoretic generalized Robinson–Foulds metrics for comparing phylogenetic trees](#). *Bioinformatics*, 36(20):5007–5013.
- Peter H.A. Sneath and Robert R. Sokal. 1973. Unweighted pair group method with arithmetic mean. *Numerical Taxonomy*, pages 230–234.
- Adam St Arnaud, David Beck, and Grzegorz Kondrak. 2017. [Identifying cognate sets across dictionaries of related languages](#). In *Proceedings of the 2017 Conference on Empirical Methods in Natural Language Processing*, pages 2519–2528, Copenhagen, Denmark. Association for Computational Linguistics.
- Mike A. Steel and David Penny. 1993. [Distributions of Tree Comparison Metrics—Some New Results](#). *Systematic Biology*, 42(2):126–141.

A Supplemental Material

A.1 Preserving the Ethnologue Tree Topology

Our previous experiments compared algorithmically-constructed trees (UPGMA and NJ) built using TDA-based distance matrices against the Ethnologue reference trees on identical sets of languages. A possible objection to this approach is that the reference trees are generally much shallower than those constructed by the algorithms, perhaps affecting our evaluation.

Thus we investigated an optimization procedure to construct TDA-based trees consistent with the reference tree topology. Instead of constructing a new tree, we try to find the best assignment of labels (languages) to the leaves based on the given distance matrix. A tree always yields a distance matrix between the leaves—the distance of two leaves is the length of the unique path connecting them. We set up an optimization process to find the label assignment leading to the tree distance matrix that best correlates with our given distance matrix. To compare distance matrices, we use the Pearson correlation coefficient. Therefore, if E is the tree distance matrix of the Ethnologue tree, and D is the distance matrix computing from the pipeline as described above, we want to find a permutation matrix P that maximizes the Pearson correlation coefficient between $P^T E P$ and D .

This is, however, a difficult optimization problem. To compute the Pearson correlation, the entries in the matrices are first replaced by their ranks, leading to matrices E', D' , and the coefficient is then the covariance $\text{cov}(E', D')$ divided by the standard deviations. The collection of entries does not change when we permute the matrices, so we retain the same ranks, means, and standard deviations. This means that we search for P maximizing $\langle P^T E' P, D' \rangle_F$, where E'', D'' are the matrices whose entries are ranks minus the mean of ranks, and $\langle \cdot, \cdot \rangle_F$ is the Frobenius inner product, which is the standard scalar product of the matrices viewed as unraveled vectors. This is, however, an instance of the quadratic assignment problem, which is generally NP-hard.

Our search for an optimal permutation is a naive flip-heuristic. Starting with a random permutation, we try random transpositions, and keep them if they improve the correlation. This procedure gets stuck in a local optimum after a few thousand flips. For each distance matrix, we ran this process 100 times and took the maximum of the local optima.

Our results are presented in Figure 5. Consistent with the results reported previously, we perform substantially better than chance for almost all combinations of TDA variant and tree distance metric, typically by two or more standard deviations from the mean.

A.2 Tree Similarity Metrics

To evaluate the experimental results, we need to quantitatively compare phylogenetic trees built using topological data analysis against the reference language tree from Ethnologue. Many labeled tree-to-labeled tree distances have been defined in the literature. We chose six different distances in our analysis, considering meaningfulness in our setting, availability of implementation, and efficiency of computation.

Generally there are two main directions in comparing trees. One is to define some notion of distances between pairs of leaves—e.g., the length of the shortest path connecting leaves or the distances of the closest common ancestor to either the root or to the leaves—and compare the distance matrices. This approach is not particularly well suited for our application, as reference Ethnologue tree is very flat. Nevertheless, we include one such distance.

Path distance (Farris, 1969; Steel and Penny, 1993). A path distance matrix of a tree is labeled by the leaves, and an entry is the length of the unique path in the tree that connects the corresponding two leaves. The distance of two trees is then the Frobenius distance of their path distance matrices—that is, the Euclidean distance when the matrices are unraveled into vectors.

The other option is to compare the different ways that the tree can partition its leaves into two groups by removing an edge. The first and simplest such method is the Robinson-Foulds (RF) metric (Robinson and Foulds, 1981). The distance of two trees, T_1, T_2 , with the same leaves, is the number of partitions achievable by T_1 , but not T_2 , plus the number of partitions achievable by T_2 but not T_1 ; possibly normalised to range from 0 to 1. Partitioning is intuitively a good way to measure success of our method—after all, when naively comparing a constructed tree to the reference, we argue with claims like “Slavic languages are well separated from the others”. The problem with RF is that comparing partitions on the nose is too penalizing. For example with a single swap of Portuguese with Czech in the 30-language Ethnologue tree (Figure 7), we go

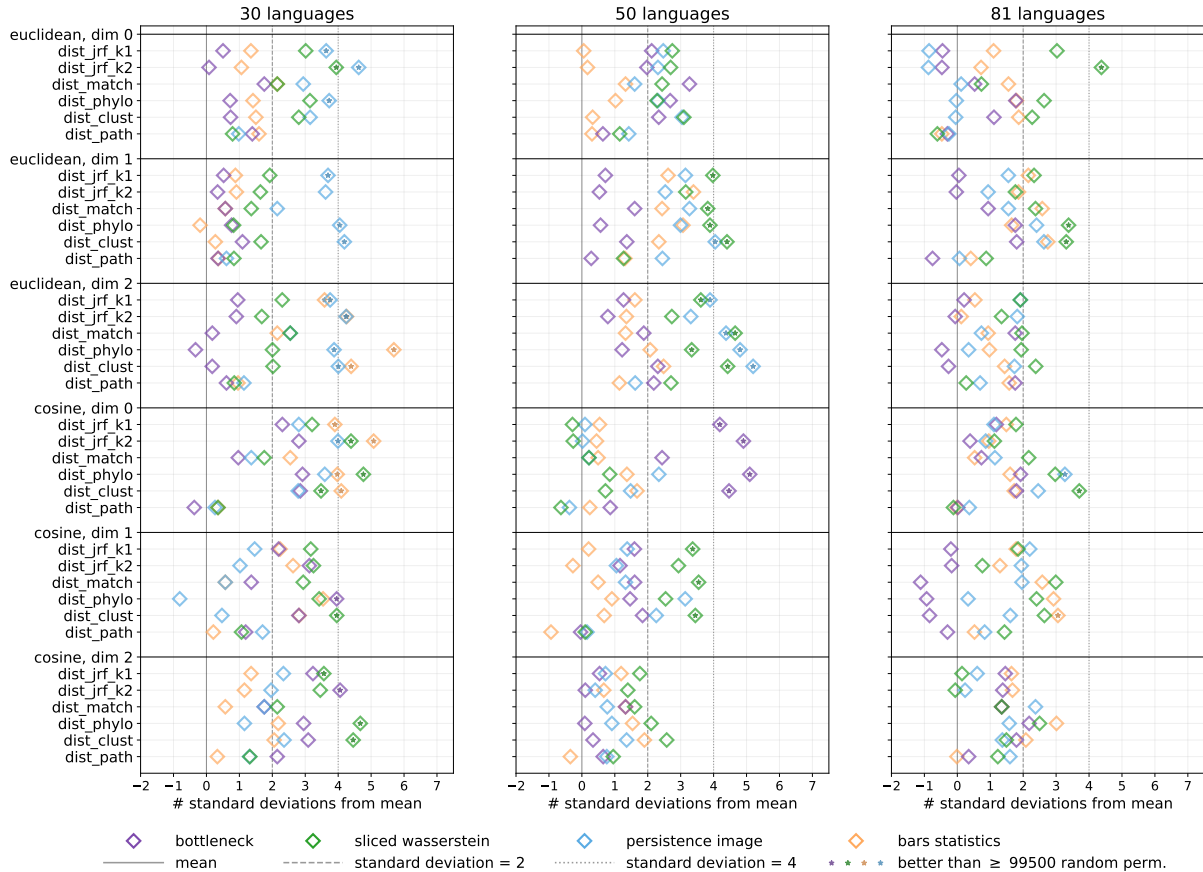


Figure 5: The statistical significance of the labelings of the Ethnologue tree that optimize distance matrix correlation (see Section A.1), for each combination of parameters described in Section 4. Each dot represents the distance of a single reconstructed labeling to the reference Ethnologue tree, and its position shows how many standard deviations away from the mean it lies in a distribution of 100,000 random labelings of the Ethnologue tree.

from distance zero to more than half of the maximum. Even reasonably similar trees can often get the maximum distance.

To fix the issue, generalizations of RF metric quantify the similarity of any pair of partitions. To compute how similar two trees are, we find the matching of the partitions defined by T_1 with the ones defined by T_2 that maximizes the sum of similarities of the matched partitions. To go from similarity to distance, we take the difference of theoretically maximal similarity and the computed similarity, and normalize to fit in the range 0 to 1. All the distances below follow the same logic, but differ in the definition of the similarity between two partitions. For the explanations, consider A_0, A_1 a partition of the leaves obtained by removing an edge from the tree T_1 , and B_0, B_1 another partition arising the same way from T_2 .

Jaccard-Robinson-Foulds distance (Nye et al., 2005; Böcker et al., 2013). JRF is a family of distances with one parameter, k . Its

name comes from using the Jaccard index: $J(A_i, B_j) := |A_i \cup B_j| / |A_i \cap B_j|$. The similarity of two partitions is defined as the bigger of the two values, $\min(J(A_0, B_0), J(A_1, B_1))$ and $\min(J(A_0, B_1), J(A_1, B_0))$, raised to the power k . As k tends to infinity, JRF distance converges to RF. In our analysis, we use $k = 1$ and $k = 2$.

Matching split distance (Bogdanowicz and Giaro, 2012; Lin et al., 2012). The matching similarity of two partitions is the maximum of $|A_0 \cap B_0| + |A_1 \cap B_1|$ and $|A_0 \cap B_1| + |A_1 \cap B_0|$. The idea is that the number of leaves minus the similarity is the number of leaves that need to be swapped in order to obtain identical partitions.

Phylogenetic and Clustering information distances (Smith, 2020). These metrics use notions from information theory to quantify similarity of partitions. The former measures the information in bits shared between the two partitions, while the latter quantifies the similarity with shared entropy.

For further details on both the intuition and the technicalities of the tree distances, see the documentation⁷ of TreeDist package for R, which we used for the computations.

A.3 P-values from Permuting Labels

Although there exist many distance metrics for comparing rooted, labeled trees, these metrics can be difficult to interpret because they conflate differences in tree topologies (e.g height and width) with differences in leaf labelings (e.g. which label pairs are siblings of each other). In our experiments with language phylogenies, we observed that the topologies of trees built from different heuristics (NJ and UPGMA) differed dramatically, and that both differed substantially in shape from both the reference tree and random trees constructed from natural agglomerative processes.

To evaluate the statistical significance of TDA-inspired trees, we propose the following procedure to mitigate impact of differing topology on our distance metrics. To evaluate how well an algorithmic tree (T) agrees with a given reference tree (R) with respect to a given distance metric $d(T, R)$, we construct a set of n random label-permuted algorithmic trees $T'(i)$, $1 \leq i \leq n$. These label-permuted trees will each have the exact same topology as T , but the leaf-labels of T be randomly and independently permuted in each $T'(i)$.

Comparing $d(T, R)$ to $d(T'(i), R)$ reflects only the differences in labeling while conserving topology. The degree to which T is better than the background of label-permuted can be assessed in two different ways. First, the rank r of the value $d(T, R)$ against the universe of n label-permuted trees yields a p-value of $(r - 1)/n$. Second, after computing the mean μ and standard deviation σ of the distribution of $d(T'(i), R)$, we can interpret $d(T, R)$ in terms of the number of standard deviations from the mean, which map directly to p-values assuming a normal distribution. We employ both techniques in the analysis to follow. The Spearman correlation of the two approaches is larger than 0.99, which indicates that we can use them interchangeably. We prefer the latter as it also takes the spread of the distribution into account, and can additionally identify meaningful p-values of statistical significance greater than $1/100,000$.

⁷<https://ms609.github.io/TreeDist/reference/index.html>

A.4 Significance Results

The result for the number of standard deviations from the mean are presented in Figure 6. Fully 451 out of 864 conditions yielded results that sat at least 2σ above the mean, with 229 at least 3σ , 74 at least 4σ , and five conditions at least 6σ above the mean, peaking at 6.87σ . For detailed breakdown see Table 3.

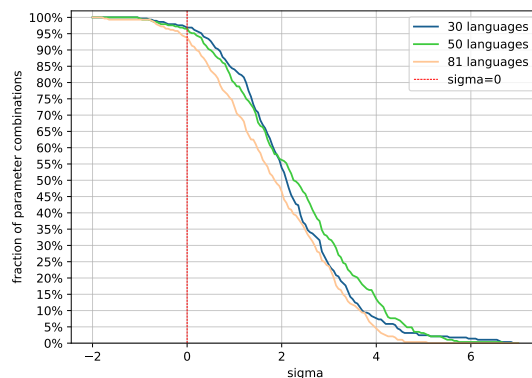


Figure 6: The fraction of parameter combinations (out of 288) in Figure 3 further away from the mean than σ standard deviations.

A.5 Evaluation of TDA Methods

To better understand which parameters perform the best, we aggregate the information from Figure 3 in two ways. In Table 1, we give the averages of standard deviations away from the mean when we fix some parameters and vary others, while in Table 2 we show the numbers of dots that performed better than 99.5% of the random permutations. In the first block of each table we compare metric for the word embedding and persistent homology dimension to compare the different distances. In the second block we compare the persistence diagram distance to compare how meaningful different topological features were. In the third block we compare tree construction algorithms.

Overall dimension 1 seems to outperform 0 and 2 for both Euclidean and cosine metric, and there is no clear winner between the two metrics. It is, however, surprising that Euclidean metric with 2-dimensional topological features is not too far behind. When we look at the persistence diagrams on Figure 9, we see that the 2-dimensional diagrams for Euclidean metric are somewhat sparse and all the features seem to be close to the diagonal. Indeed, probing all the diagrams, the maximum persistence of 2-dimensional features is roughly comparable to the smallest distance between the

embeddings of any two words for the given language. Since features can pop up or disappear at the diagonal with small perturbations of data, such low-persistent features would often be discarded as noise. Yet, in combination with bars statistics distance, the trees constructed with UPGMA algorithm based on this data are among the best performing in our analysis.

From the persistence diagram distances, sliced Wasserstein and bars statistics lead to clearly stronger results than bottleneck distance and persistence images. Bottleneck distance is expected to be subpar, as having one more or one fewer feature can already yield a large distance. It is a bit less clear why persistent images do not perform so well, especially when they should approximate 1-Wasserstein distance just as the sliced Wasserstein. One possible reason is that the method has many parameters and our choice might not be ideal—we chose range, for both birth and death, $(0, 1)$, $\sigma = .1$, for cosine; and $(0, 10)$, $\sigma = 1$, for Euclidean; grid 10×10 .

# σ from mean	j_k1	j_k2	mat	phy	clust	path	mean
Euclidean, dim 0	2.19	2.54	1.37	2.14	2.19	0.83	1.88
Euclidean, dim 1	2.74	2.57	2.33	2.74	3.10	1.14	2.43
Euclidean, dim 2	2.38	2.17	2.17	2.38	2.74	0.76	2.10
cosine, dim 0	2.19	2.19	1.53	2.63	2.58	0.62	1.95
cosine, dim 1	2.41	2.14	2.58	3.28	3.27	1.46	2.52
cosine, dim 2	1.72	1.36	1.76	2.89	2.71	0.93	1.90
bottleneck	1.80	1.70	1.57	2.28	2.36	0.93	1.78
sliced Wasserstein	2.63	2.49	2.40	2.95	3.12	1.05	2.44
persistence image	2.25	2.17	1.69	2.21	2.38	0.88	1.93
bars statistics	2.40	2.28	2.17	3.26	3.19	0.97	2.38
nj	2.20	2.14	1.70	2.48	2.65	0.90	2.01
upgma	2.34	2.18	2.21	2.88	2.87	1.02	2.25

Table 1: Averages of the values presented in Figure 3 (number of standard deviations away from the mean). In each block we fix one of the parameters, and aggregate over all others.

# ≥ 99500	j_k1	j_k2	mat	phy	clust	path	sum
Euclidean, dim 0	6	6	2	6	4	0	24
Euclidean, dim 1	8	4	4	7	12	0	35
Euclidean, dim 2	7	3	8	6	9	0	33
cosine, dim 0	2	1	2	5	7	0	17
cosine, dim 1	5	3	6	13	14	1	42
cosine, dim 2	2	0	4	10	10	0	26
bottleneck	4	2	3	9	12	0	30
sliced Wasserstein	10	7	9	14	19	0	59
persistence image	5	3	4	7	8	0	27
bars statistics	11	5	10	17	17	1	61
nj	12	7	8	15	21	0	63
upgma	18	10	18	32	35	1	114

Table 2: The number of dots in Figure 3 corresponding to parameters that performed better than 99,500 random permutations of the tree leaves (labeled by star in the figure). The total number of dots for a fixed distance that meet the parameters in each block is 24, 36 and 72, respectively.

full fig	all	jrf_k1	jrf_k2	match	phylo	clust	path
total	864	144	144	144	144	144	144
$\sigma > 1$	681	121	111	117	134	134	64
$\sigma > 2$	451	84	74	72	99	103	19
$\sigma > 3$	229	36	41	29	59	63	1
$\sigma > 4$	74	13	15	7	17	22	0
$\sigma > 5$	17	2	4	1	5	5	0
$\sigma > 6$	5	0	2	0	2	1	0
30 lang	all	jrf_k1	jrf_k2	match	phylo	clust	path
total	288	48	48	48	48	48	48
$\sigma > 1$	242	43	40	43	44	45	27
$\sigma > 2$	155	31	31	24	26	30	13
$\sigma > 3$	69	12	19	11	13	13	1
$\sigma > 4$	22	3	4	3	4	8	0
$\sigma > 5$	7	1	1	1	2	2	0
$\sigma > 6$	4	0	1	0	2	1	0
50 lang	all	jrf_k1	jrf_k2	match	phylo	clust	path
total	288	48	48	48	48	48	48
$\sigma > 1$	230	40	36	39	47	46	22
$\sigma > 2$	162	28	26	24	40	40	4
$\sigma > 3$	92	16	17	10	23	26	0
$\sigma > 4$	39	8	9	2	10	10	0
$\sigma > 5$	9	1	3	0	3	2	0
$\sigma > 6$	1	0	1	0	0	0	0
81 lang	all	jrf_k1	jrf_k2	match	phylo	clust	path
total	288	48	48	48	48	48	48
$\sigma > 1$	209	38	35	35	43	43	15
$\sigma > 2$	134	25	17	24	33	33	2
$\sigma > 3$	68	8	5	8	23	24	0
$\sigma > 4$	13	2	2	2	3	4	0
$\sigma > 5$	1	0	0	0	0	1	0
$\sigma > 6$	0	0	0	0	0	0	0

Table 3: The number of parameters in Figure 3 with value greater than a given threshold.

full fig	all	jrf_k1	jrf_k2	match	phylo	clust	path
total	864	144	144	144	144	144	144
top 10.00%	613	113	102	98	121	128	51
top 5.00%	484	90	75	76	102	112	29
top 1.00%	255	39	34	42	65	72	3
top 0.50%	177	30	17	26	47	56	1
top 0.10%	57	10	4	10	14	19	0
top 0.05%	32	5	3	5	9	10	0
top 0.01%	10	1	2	2	2	3	0
30 lang	all	jrf_k1	jrf_k2	match	phylo	clust	path
total	288	48	48	48	48	48	48
top 10.00%	217	40	39	33	36	44	25
top 5.00%	172	34	33	26	28	34	17
top 1.00%	75	13	15	14	12	18	3
top 0.50%	46	11	5	9	9	11	1
top 0.10%	16	2	1	3	4	6	0
top 0.05%	9	1	1	3	2	2	0
top 0.01%	5	1	1	1	1	1	0
50 lang	all	jrf_k1	jrf_k2	match	phylo	clust	path
total	288	48	48	48	48	48	48
top 10.00%	212	38	33	34	47	43	17
top 5.00%	169	30	25	25	41	41	7
top 1.00%	100	17	15	13	27	28	0
top 0.50%	74	13	10	9	18	24	0
top 0.10%	29	6	3	3	8	9	0
top 0.05%	18	3	2	1	6	6	0
top 0.01%	3	0	1	0	1	1	0
81 lang	all	jrf_k1	jrf_k2	match	phylo	clust	path
total	288	48	48	48	48	48	48
top 10.00%	184	35	30	31	38	41	9
top 5.00%	143	26	17	25	33	37	5
top 1.00%	80	9	4	15	26	26	0
top 0.50%	57	6	2	8	20	21	0
top 0.10%	12	2	0	4	2	4	0
top 0.05%	5	1	0	1	1	2	0
top 0.01%	2	0	0	1	0	1	0

Table 4: The number of parameters in Figure 3 with distance smaller than the given percentage of the 100,000 permutations.



Figure 7: The reference Ethnologue language phylogenetic trees (Lewis et al., 2024) employed in this study, for sets of the most popular 30, 50 and 81 Indo-European languages with FastText word embeddings.

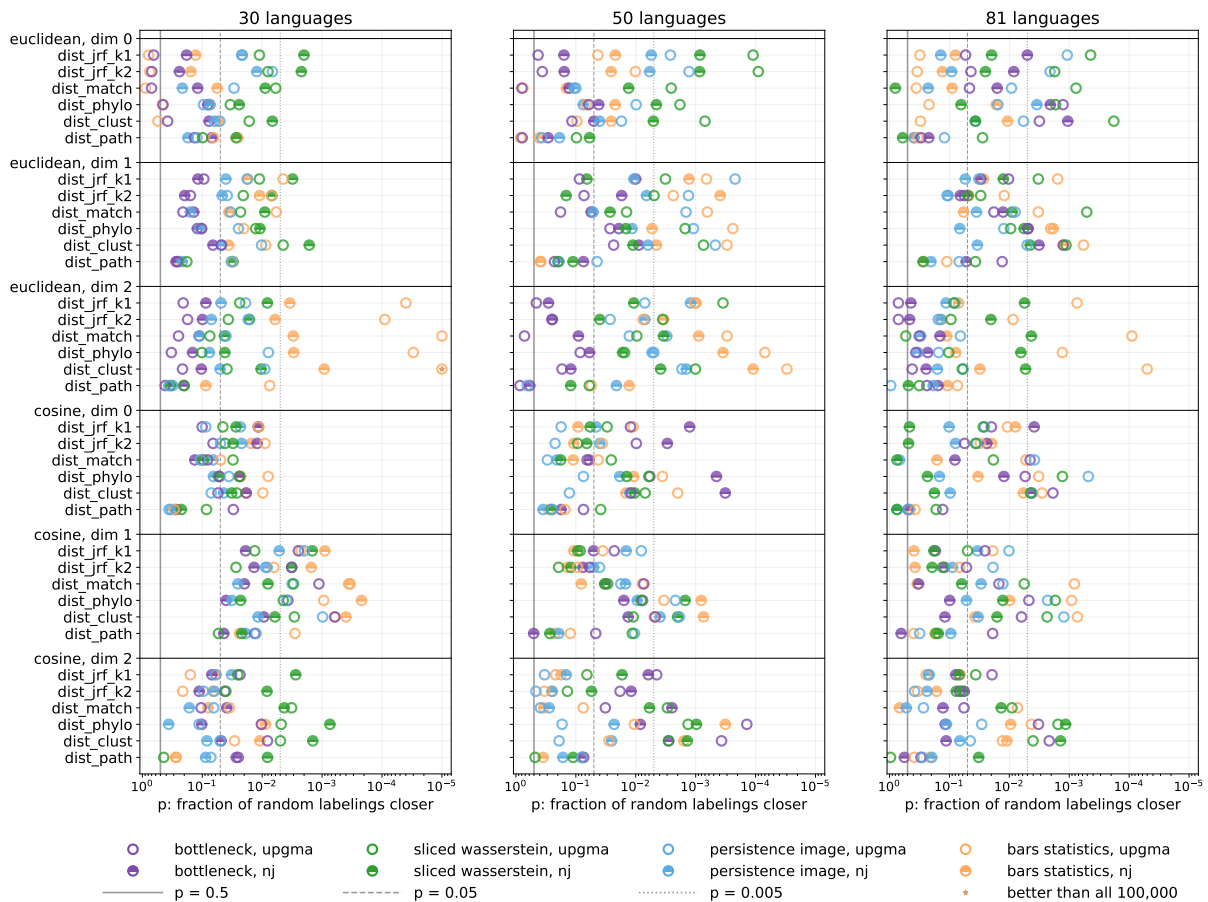


Figure 8: The statistical significance of TDA trees for 30, 50, and 81 languages against the Ethnologue reference for trees reconstructed by UPGMA and NJ for each combination of parameters described in Section 4, as in Figure 3. Each dot represents the distance of a single reconstructed tree to the reference, and its position shows what fraction of 100,000 random permutations of the tree’s leaves lead to smaller distances.

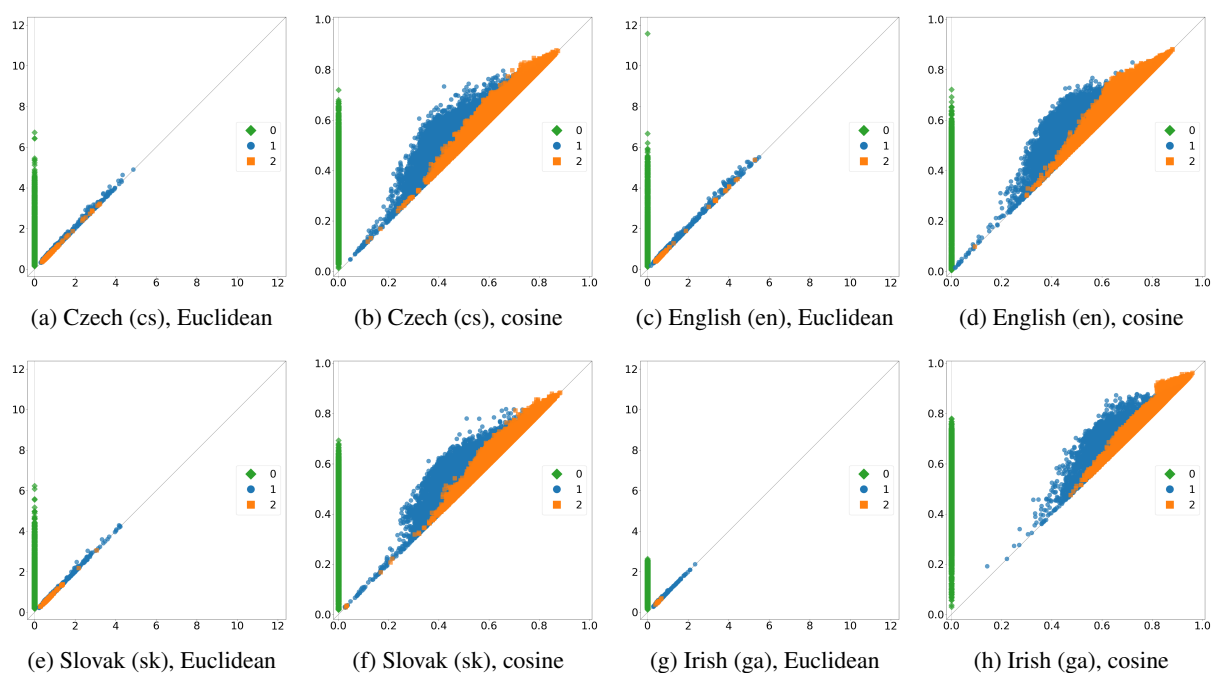


Figure 9: Eight persistence diagrams for language embeddings analysed in this paper including Czech and Slovak, which are very closely related, and English and Irish, which belong to distant branches (Germanic and Celtic) of the Indo-European family. For each language we show diagrams for distinct Euclidean and cosine metrics. Each diagram shows features for dimensions 0, 1 and 2, that is, connected components, loops, and 2-spheres.